Investigation on the Effect of the $CdCl_2$ Treatment on CdTe Thin-film Solar Cells of Variable Thickness Fabricated Using Combinatorial Pulsed Laser Deposition

By

Ali Saber Kadhim

Submitted to the graduate degree program in Physics and astronomy and the Graduate Faculty of the University of Kansas in partial fulfillment of the requirements for the degree of Master of Arts.

_____

Chairperson: Judy Wu, Ph.D.

_____

Wai-Lun Chan, Ph.D.

_____

Cindy Berrie, Ph.D.

Date Defended: June 15th, 2015

The Thesis Committee for Ali Saber Kadhim

certifies that this is the approved version of the following thesis:

Investigation on the Effect of $CdCl_2$ Treatment on CdTe Thin-film Solar Cells of Variable Thickness Fabricated Using Combinatorial Pulsed Laser Deposition

_____

Chairperson: Judy Wu, Ph.D.

Date Defended: June 15th, 2015

Abstract

Cadmium Chloride ($CdCl_2$) post annealing process has significant impacts on the performance of the CdS/CdTe solar cells since it affects the microstructure, crystallinity and charge carrier doping in CdTe films and also the CdS/CdTe p-n junction formed through S and Te interdiffusion at the junction interface. Therefore, this process has been investigated extensively during the past two decades, and has been optimized for polycrystalline CdS/CdTe thick film solar cells, in which the CdTe thickness is typically in the range of 3-8 μm. Nevertheless, the recent effort to develop cost-performance balanced thin film CdS/CdTe solar cells (with CdTe thickness on the order of 1 μm or less) has encountered difficulties through direct applications of the thick-film $CdCl_2$ post annealing process. These difficulties stem from the large CdTe grain sizes typically in the range of microns in the thick film case. Grain boundaries between such large grains result in through-thickness shorts when the CdTe film thickness is comparable to or smaller than the grain size. Overcoming these difficulties to achieve precise controls of grain morphology, crystallinity and CdS/CdTe interface is important to high-performance CdS/CdTe thin film solar cells and will be the main objective of this thesis. In order to accelerate the study, a combinatorial Pulsed Laser Deposition technique (cPLD) was developed for deposition of CdTe films with different thicknesses on each sample to elucidate important physical properties of Cl diffusion through the selected thickness range at a given $CdCl_2$ annealing condition. Two sets of samples A and B of CdTe solar cells of multiple thicknesses of 1.5, 1.25, 1.0, and 0.75 μm have been fabricated by using cPLD. Sample A was completed without $CdCl_2$ treatment as a reference, and sample B was treated with $CdCl_2$ in different durations (10, 12, 15, and 17 min) at 360 ^oC in mixed vapor of O_2 and Argon (25 sccm:100 sccm). The sample that was treated at 15 minutes $CdCl_2$ showed the best performance

in all thickness range 0.75-1.5 μm. Through comparisons between the two types of samples with and without $CdCl_2$ annealing, it became obvious that the $CdCl_2$ treatment promotes the recrystallization and grain growth of CdTe films, which led to improvements in the performance of the solar cells. In addition, different performance between the variable thicknesses of CdTe on the same sample was studied, and the highest efficiency 5.3% was obtained from the 0.75 μm.

Acknowledgements

I express my sincere thanks and heartfelt gratitude to my advisor Dr. Judy Wu, for giving me this opportunity to work with her. I would like to thank her for her valuable advices and suggestions throughout my thesis. I am also thankful to Dr. Wai-Lun Chan and Dr. Cindy Berrie for serving on my thesis committee. I would like to take this chance to thank Dr. Guanggen Zeng for his grateful suggestions and comments. I am very thankful to my colleagues both of Alaa Al_ mebir and Paul Harrison. My special thanks to my friend Alaa for his advice and support. I extend heartfelt thanks to my parents, wife, and other friends for their supports and encouragements without which this work would not have been done.

Table of Contents

List of Figures

List of Tables

Chapter 1. Introduction

1.1 Solar Cell's History

In 1839, the photovoltaic effect was discovered by French scientist Edmond Becquerel. He made an electrolytic cell of silver, coated with a platinum electrode. The cell was placed into an electrical solution. What Edmond Becquerel observed was that the electric current can be increased when the cell is exposed to the light[1, 2]. In 1873, the photoconductivity of selenium was observed by Smith. Three years later, Adams and Day also observed the photovoltaic effect in the selenium [3]. In 1914, 1% solar conversion efficiency was achieved from the selenium cell. A thin film of copper-copper oxide structure has also shown the photovoltaic effects. In addition, in the same year (1914) Goldman and Brodsky noticed that the energy barrier existed in both selenium and copper-copper oxide solar cells [2, 3]. In the period between the 1950s and 1960s, there were a lot of developments in silicon solar cells. For instance, in 1954, Chapin, Fuller, and Pearson reported the first solar cell made from a silicon single-crystal, and the highest conversion efficiency was 6% [4]. In the same year, also 6% conversion efficiency was reported from cadmium sulfide and cuprous sulfide [3, 5]. Many thin films, such as indium phosphide, gallium arsenide, and cadmium telluride have attracted the attention of many researchers due to this theoretical work, which showed that the higher efficiency can be produced from these materials[6]. The solar cells received huge interest as alternative sources of energy; so many materials have been explored and developed as thin film materials. Researchers sought to reduce the cost and maintain the availability of these materials. The best thin film materials that have been used in the solar cell devices are amorphous silicon (α-Si), cadmium telluride (CdTe), and copper indium diselenide (CuInSe2) [3]. By contrast, the production of silicon crystalline and polycrystalline is too expensive and may reach 1.15$/W after many optimizations. However, the

small amount of material and low cost make the thin film solar cells the preferable materials as an alternative energy. Moreover, the cost of the CdTe solar cell might reach 0.95$/W [7].

1.2 The Principle of Solar Cell

Conversion of energy from incident photons (sunlight) directly into electricity (current) using solar cells is called the process of photovoltaics. Basically, this process is based on the p-n junction device. The semiconductor materials can exhibit the photoelectric effect which means that when the light is absorbed by these materials, the incident photons create the electron-hole pair [3]. In other words, if the incident photon has energy greater than the energy of band gap, it will be absorbed inside the semiconductors. Therefore, the electron will be excited from the valance band to the conduction band leaving behind a hole. In addition, if the semiconductor has direct band gap, the electron will easily reach to the conduction band. However, indirect band gap needs some momentum to do so. Figure 1 shows this process.

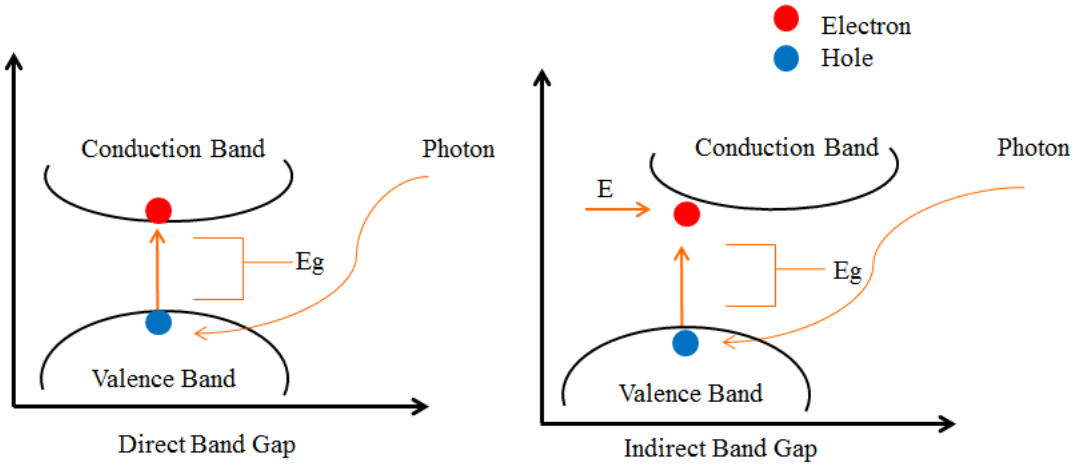

Figure 1: Band gap of semiconductor.

The majority of carriers are holes and electrons inside the p and n types respectively. The two semiconductors should be brought together to create a p-n junction. In addition, there are two types of p-n junctions. The first one is called Heterojunction in which two different semiconductors form the junction. One of them is p type and the other is n type. The Homojunction is the second type of the p-n junction in which the same semiconductors with different doping to create a p and n types are brought together [8, 9].

Figure 2 shows the different concentrations between the two regions of p-n junction; the electrons move from n-type to the p-type region.

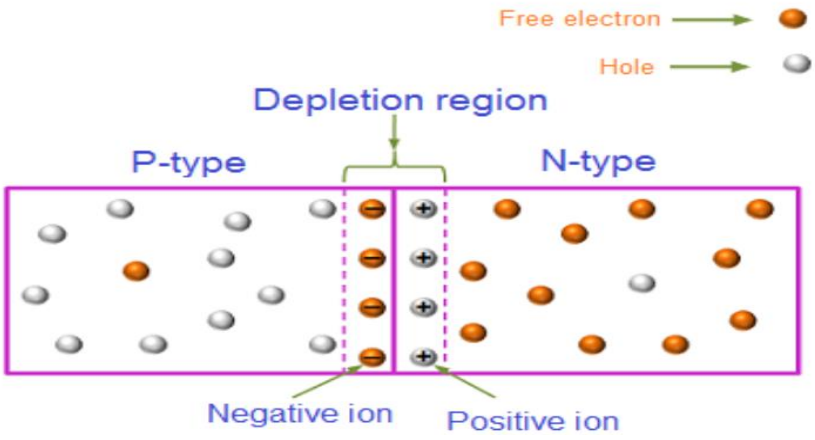

Figure 2: Single p-n junction[10].

The holes move from the p- type to the n- type. If the holes and electrons were not charged, the process of diffusion would not stop until the concentration of holes and electrons on both sides reach equilibrium state. The result of these movements is to form the p-n junction. Figure 2 also indicates that when the electron moves to the p-type part, it will leave behind a fixed positive ion. Likewise, when the hole moves to the n-type, it will leave a fixed negative ion. This means that the negative and positive charges appear on the p and n type sides respectively. As a result,

an electric field will be created and pointed from the positive side, which was formed in the n-type to the negative side of the material. Therefore, the charge carriers are going to move in one direction. The new layer which is formed through this process near the junction is called the space charge or the depletion region because it is depleted most of the free carriers [3, 8].

Chapter 2. Technical Aspects of CdS/CdTe Solar Cells

2.1 CdTe Solar Cells History

Since the 1950s, Cadmium Telluride (CdTe) has been known as one of the strongest semiconductor candidates that has been used in the fabrication of thin film solar cells. CdTe has many advantages for thin film solar cell applications, including a direct bandgap (~ 1.5 eV), a high absorption coefficient (up to 10^5/cm), and it can be doped n-type or p-type[11]. In 1963, it was observed that the conversion efficiency could be increased from 5% to 8% by using Cadmium Sulfide as a window layer[12]. In 1980, CdS/CdTe solar cells were made by using Close Spaced Sublimation technique (CSS), and 10% conversion efficiency was achieved[13]. Solar cells were scaled up to produce large area products using transparent conducting oxide (TCO) as the front electrode in a solar cell. In 1992, 15% conversion efficiency was achieved by adding a buffer layer (tin oxide) between TCO and CdS to allow the thickness of CdS to be reduced to less than 100 nm to improve the shorter wavelengths. About 20% of light which has energy greater than 2.42 eV could be blocked by using thick CdS[14]. Achieving higher electric conversion efficiencies of CdS/CdTe solar cells requires a Cadmium Chloride ($CdCl_2$) treatment[15]. This treatment, which is used on CdTe, is found to be extremely important in different aspects, such as helping in grain growth, blocking the channels or pinholes, and increasing the majority carriers in CdTe [16-18]. CdTe is a compound material of cadmium and telluride (Cd + Te), but if the production levels of Te increase gradually, then the availability of this material will be reduced [19]. Therefore, a lot of recent research has been focused on reducing the thickness of CdTe, which in addition to protecting Te reserves, would also decrease the device cost [20-22]. In 2006, a group from Toledo University reduced the thickness of CdTe to less than 1μm, and 11.8 % conversion efficiency was achieved by controlling the $CdCl_2$

conditions. Since then several attempts have been made, including reducing the thickness of both CdTe and CdS, adding a buffer layer to block the pinholes, and using $CdCl_2$ to reduce the recombination. The highest conversion efficiency of the CdS/CdTe so far is 18-20% [23, 24].

2.2 Structure of the CdTe Thin Film Solar Cell

Figure 3 shows a basic structure of the CdS/CdTe solar cell; generally, the structure of the CdS/CdTe solar cell is two semiconductor materials. One of them is p-type which is represented by CdTe and called the absorption layer. The other one is n-type material which is represented by CdS and acts as a window layer.

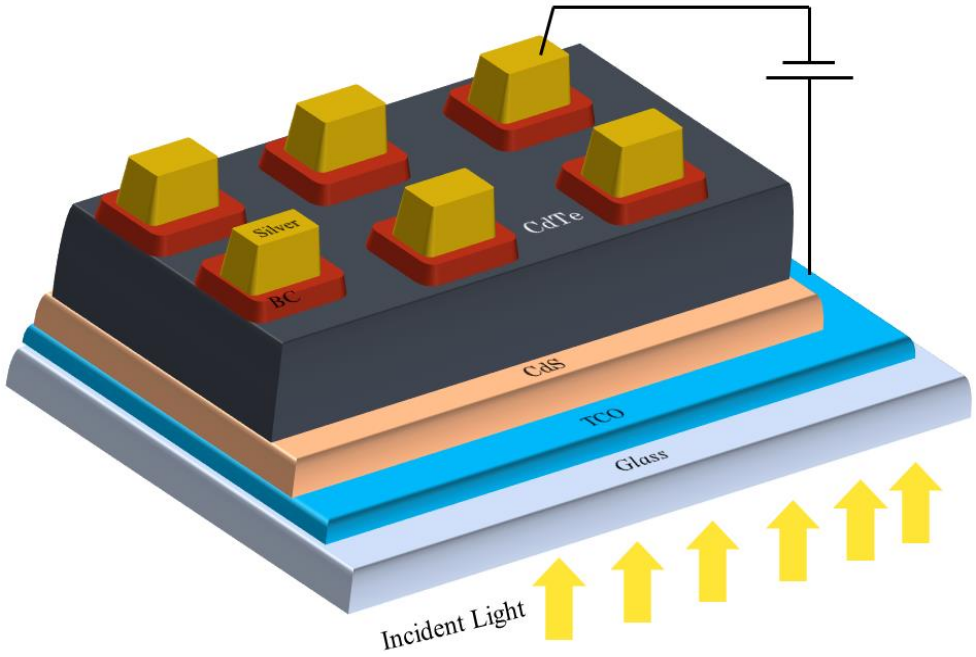

Figure 3: Structure of CdS/CdTe solar cells.

These two semiconductors come together to create a p-n junction. The CdS is deposited on glass which is coated by a transparent conductive oxide (TCO), such as indium tin oxide

(ITO) or fluorine tin oxide (FTO) to provide a front contact of the cell. The main reason to use the glass is to support the structure of the cell. Furthermore, after depositing the CdTe on the CdS, an electrode (silver, Gold, or Copper) is required to provide a contact to the cell. However, CdTe has a work function higher than the work function of the electrode. So researchers have used a back contact which is deposited on the CdTe to reduce the Schottky barrier between the CdTe semiconductor and the metal, and then the electrode will be deposited on the back contact.

As can be seen in figure 4, when the light inters the p-n junction, there are three important regions will be formed, generation, charge separation, and collection regions.

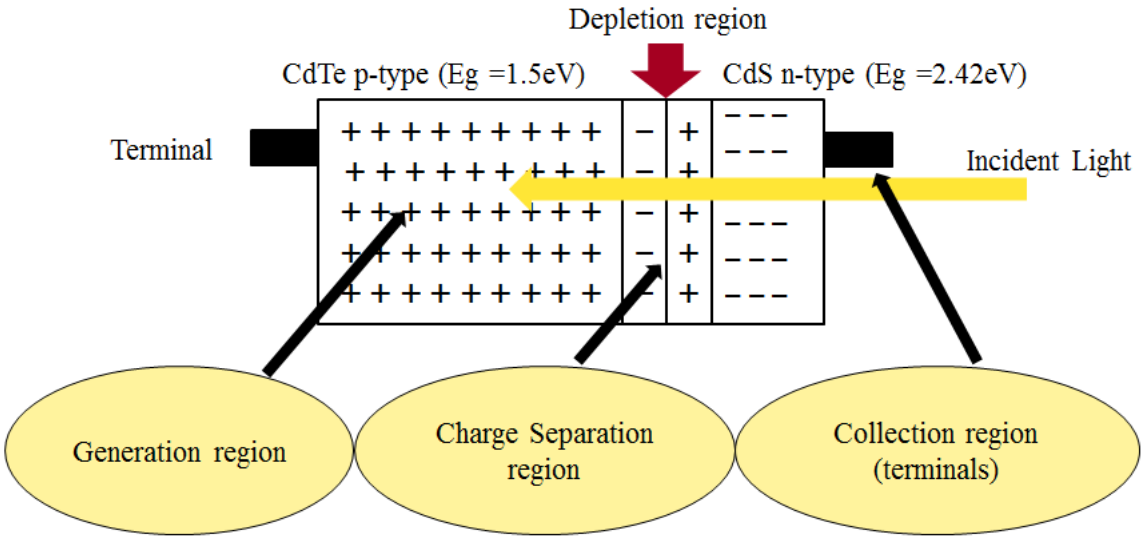

Figure 4: Diagram of the p-n junction after entering the light.

2.2.1 Electrical Front and Back Contacts

The front and back contacts are extremely important in the solar cell structure because they provide an electrical contact. The front contact is called the transparent conducting oxide (TCO),

which has a very high transparency, a very low absorption, and the sheet resistance is no more than (10 Ω/square). The material that has been used as a TCO is tin oxide, and because of its low conductivity, it is doped with fluorine or indium, and it will form fluorine tin oxide (FTO) and indium tin oxide (ITO) respectively [25, 26]. On the other hand, there is another contact, which is called the back contact, occurs between the p- type CdTe semiconductor and the metal electrode. However, making a direct contact between metal and semiconductor may create a Schottky barrier. The work function in the metal is fixed, but in the semiconductor, it can be controlled by doping [3]. The best way to reduce this resistance is to make the surface of CdTe Te-rich by using chemical etching. The etching process is used to remove contaminants from the surface as well as make a Te-rich surface for better ohmic contact.[27] This is a matter of optimization between the CdTe, back contact, and electrode and studies are already underway to resolve this issue.

2.2.2 Semiconductor Window Layer (CdS)

The p and n type semiconductor materials which have been used in the solar cell device act as absorption and window layers, respectively. The polycrystalline CdS semiconductor acts as a window layer in which photons pass into the absorption layer CdTe. The CdS semiconductor has band gap energy of (2.42 eV). The disadvantage of CdS is that the band gap is not large enough to let more photons pass through to the absorption layer. Thus the photons that have energy greater than the band gap of CdS may not be able to reach the CdTe absorber. Therefore, reducing the thickness of the CdS as much as possible is required to increase the transparency to allow more shorter wavelength photons to the absorption layer [20]. One strategy employed by some researchers uses a buffer layer, such as Zinc tin oxide (bandgap ~3.37 eV) before the CdS. This composite ZnO/CdS window replaces a part of smaller bandgap CdS with larger bandgap

ZnO for better window transparency. Generally, the buffer layer should have a band gap greater than the band gap of CdS to increase the band gap of CdS by diffusion [28].

2.2.3 Semiconductor Absorption Layer (CdTe)

Cadmium Telluride (CdTe) is one of the most important semiconductors and has been used as an absorption layer in the photovoltaic solar cell. Although the CdTe has many advantages for thin film solar cell applications including direct bandgap ($\sim$ 1.5 eV) and high absorption coefficient (up to 10^5/cm), it also has disadvantages. For instance, CdTe is a compound material of cadmium and telluride (Cd + Te), but if the production levels of Te increase gradually, then the availability of this material will be reduced [19]. Therefore, in order to avoid the reduction in the Te, most researchers have tried to reduce the thickness of the CdTe solar cell which also decreases the cost [20-22]. Therefore, reducing the thickness of the CdTe solar cell is an important process to address the issue of material sustainability and reduction of the solar cell cost. In other words, fabricating a thick film solar cell consumes a large amount of materials and requires a particular process, but a small amount of materials and a simple process are enough to develop a thin film solar cell [21, 22].

There are several materials that have been used as thin film solar cells, such as amorphous silicon (α-Si), copper indium diselenide (CuInSe2), and CdTe, which act as absorption layers. Table 1 is a comparison among these three materials; it is obvious that the CdTe is the strongest candidate among them as an absorption layer based on considerations of electronic structures and cost [3].

Table 1: Comparison among Cadmium Telluride (CdTe), Amorphous Silicon (α-Si), and Copper Indium Diselenide (CuInSe2)

Copper Indium Diselenide (CuInSe2)	Amorphous Silicon (α-Si)	Cadmium Telluride (CdTe)
The band gap 1.02 eV	The band gap 1.7 eV	The band gap 1.5 eV
Direct band gap	Direct band gap	Direct band gap
absorption 2 µm absorbs most of the light	absorption 5 µm absorbs most of the light	absorption 1 µm absorbs 90% of the light
Polycrystalline	Amorphous	Polycrystalline
Indium is very expensive.	It is cheap.	It is cheap.

2.3 Parameters of the Solar Cell

The measurements of the Current–Voltage (J-V) for a solar cell provide the most important information about the performance of the solar cell. From the J-V curve, several parameters can be obtained, such as the short circuit current (J_{sc}), open circuit voltage (V_{oc}), fill factor (FF), and the conversion efficiency (η). In addition, information about the series and shunt resistances also can be provided from the J-V curve. The quality of the materials and the optimal solar cell design can be obtained by measuring an important parameter, which is called the external quantum efficiency (EQE). EQE represents the ratio between the numbers of electrons collected by the solar cell to the number of photons incident on the solar cell [3, 29].

2.3.1 Short Circuit Current (J_{sc}) & Open Circuit Voltage (V_{oc})

One of the parameters which can highly affects solar cell performance is the short circuit current, which is the highest current in the solar cell when the voltage into the cells equals zero (see figure 5). Basically, the (J_{sc}) is represented by the following equation:

$$J_{sc} = \frac{I_{SC}}{A} \quad (mA/cm^2).$$

(J_{sc}) and (A) are the current density and the area of the solar cell respectively [3, 30].

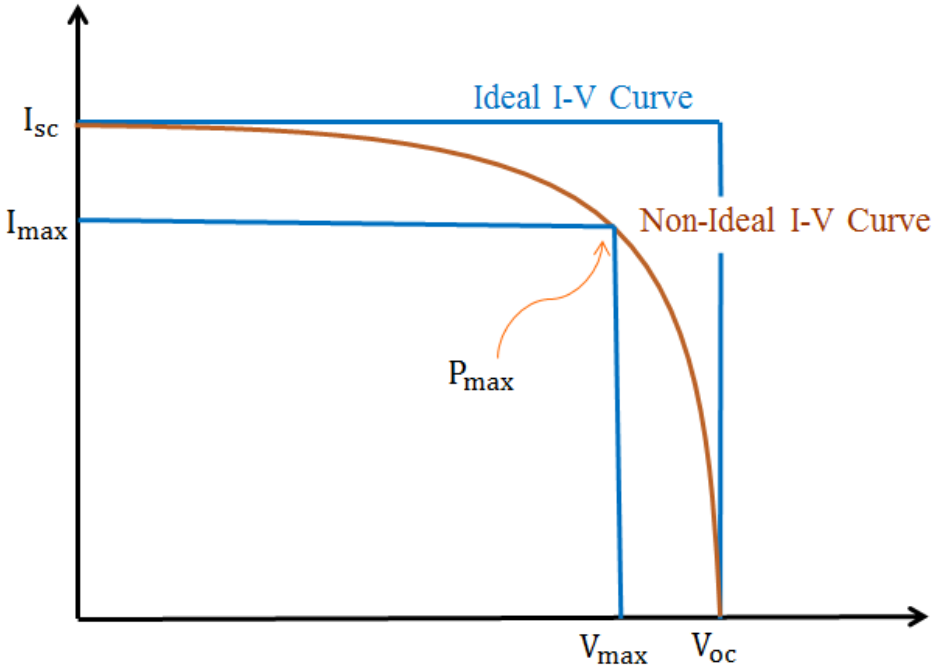

Figure 5: Current-Voltage (I-V) curve.

In addition, there are several parameters which can influence the short circuit current itself, such as incident light intensity, and the optical properties of the solar cell (absorption and reflection). However, the major effect on the J_{sc} is the recombination which occurs due to the short life time

of the electrons [30]. Figure 5 also shows the open circuit voltage (V_{oc}), which is the highest voltage through the solar cell when the current equals zero [31].

2.3.2 Fill Factor (FF)

One of the parameters that can be directly determined from the I-V curve is the fill factor (FF), which is defined as the ratio of the power in the maximum value (P_m=I_m.V_m) to the product of the short circuit current (J_{sc}) and the open circuit voltage (V_{oc}). The major effect on the FF is the recombination [32]. The equation below represents the FF:

$$FF = \frac{P_m}{V_{oc} * I_{sc}} = \frac{I_m * V_m}{V_{oc} * I_{sc}}$$

2.3.3 Power Conversion Efficiency of the Solar Cell (η)

The power conversion efficiency is the key parameter of the solar cell which can be used to determine the best performance of one solar cell to another. The efficiency is the ratio of the output power, which is electricity from the solar cell, to the input power, which is incident photons (light) from the sun. It can be calculated from the following equation [3, 33]:

$$\eta = \frac{P_{out}}{P_{in}} = \frac{V_{oc} I_{sc} FF}{P_{in}}$$

The standard spectrum (P_{in}) is $100 mW/cm^2$.

2.4 Series and Shunt Resistances

There are two types of resistances in the solar cell which must be in the right ranges to not cause a reduction in the efficiency. One of them is a series resistance (R_s) which occurs due to the contact between the metal and the semiconductor. An ideal value of R_s is zero. While it is

difficult, the experimental efforts have been put to minimize the R_s and therefore the power loss it causes. The other resistance is called a shunt resistance (R_{sh}) which is the resistance at the p-n junction, which is infinite for a perfect p-n junction. A finite R_{sh} on the solar cell implies an alternative path for the current, which leads to degraded solar cell performance. Both of the series and shunt resistances have a major effect on the solar cell's fill factor due to the power dissipation [3, 34, 35]. The series and shunt resistances can be estimated from the J-V curve's slope; the effect that appears near the short circuit current gives us information about the R_{sh}. Moreover, the R_s effect can appear near the open circuit voltage. Figure 6 shows the R_s and R_{sh} [34, 35].

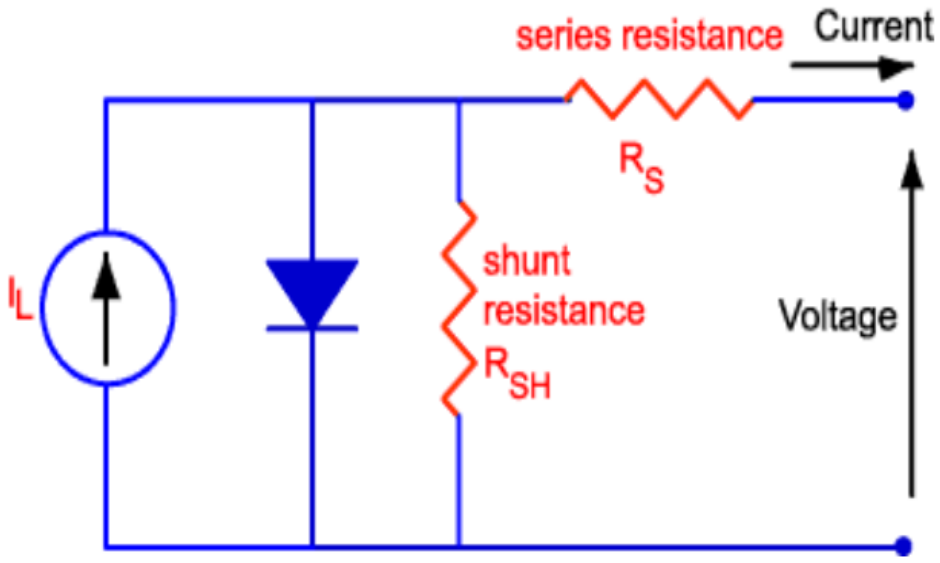

Figure 6: Series and shunt resistances.

2.5 External Quantum Efficiency (EQE)

The ratio of the number of charge carriers collected by the solar cell to the incident photons flux on the solar cell is the external quantum efficiency (EQE). The QE for an ideal solar

cell means that each photon from the incident photons flux will create an electron-hole pair, and then the pair might be separated into the depletion region and collected on the top of the cell. However, it is difficult to get an ideal QE solar cell because the incident photons have different energies, so not every photon can generate an electron-hole pair. In other words, if the photon has energy greater than the band gap of the semiconductor, the (e-h) pair will be created; otherwise, it will not. As a result, the EQE depends on the photon absorption, efficiency of charge separation and collection [3, 29]. Figure 7 shows the ideal and non-ideal EQE of CdS/CdTe solar cell as an example.

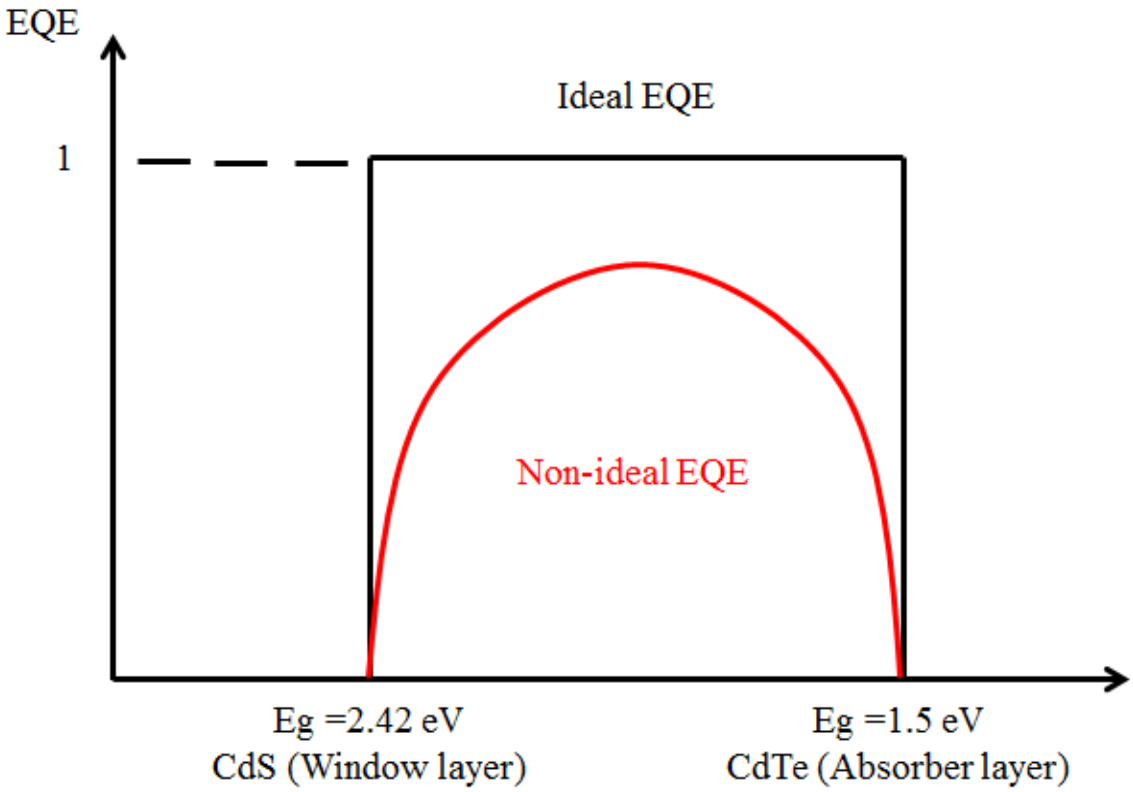

Figure 7: Ideal and non-ideal EQE of CdS/CdTe solar cell.

Chapter 3. Experimental

3.1 Experimental

Different techniques have to be applied in order to determine the performance and properties of the solar cells. Often, it is difficult to correlate the performance of a solar cell with its microstructure by measuring one characteristic. Therefore, in order to understand performance limiting factors of the solar cells, multi scale characterization from microscopic to macroscopic must be taken. In this study, there are three major steps involved in CdS/CdTe solar cell fabrication and characterization. First, the fabrication technique, in which Pulsed Laser Deposition technique, Cadmium Chloride ($CdCl_2$) treatment, Bromine etches, and electrical back contacts have been used to fabricate a complete cell. Next, Atomic force microscopy (AFM) and Raman spectroscopy have been utilized to measure the microstructure (morphology and crystallinity) of the materials in the solar cell. Finally, electrical measurements were taken of the current density-voltage (J-V) and the quantum efficiency.

3.2 Fabrication CdS/CdTe Solar Cell

In order to fabricate a complete solar cell, there are several necessary steps, such as deposition technique, the $CdCl_2$ treatment, bromine etches, back contact with electrode. Once completed, the structural and electrical measurements can be applied to determine the performance of the solar cell.

3.2.1 Combinatorial Pulsed Laser Deposition (cPLD) Technique

There are numerous methods that have been used to deposit CdS/CdTe semiconductors to produce solar cells. Physical Vapor Deposition (PVD), Close-Space Sublimation (CSS), Vapor Transport Deposition (VTD), Sputter Deposition, Metal Organic Chemical Vapor Deposition

(MOCVD), Spray Deposition, and Pulsed Laser Deposition (PLD) are some of the methods that have been used to fabricate solar cells [36]. In addition, these methods have been improved and developed by companies of solar cells and some researchers. In this study, the method that was utilized is the combinatorial Pulsed Laser Deposition (cPLD) as shown in figure 8.

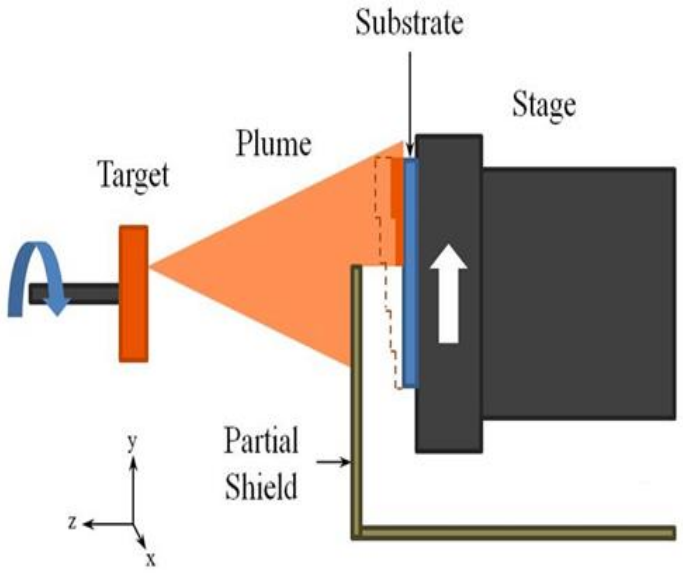

Figure 8: A depiction of the combinatorial PLD process which allows different thicknesses to be deposited on a single substrate.

The PLD system consists of a 248 nm KrF excimer laser with 20 ns laser pulse duration. The absorber and window layer targets are mounted inside of a vacuum chamber on rotating stands that allow for both targets to be moved into the path of the laser and rotation about the axis of the targets facilitates uniform ablation of the target surface.[37-41]. The substrate stage is mounted into the chamber across from the targets with a distance of 5.5 cm separate the two. The scanning stage has two axes of movement so that it can move in any motion desired that is perpendicular to the laser plume axis. Two external stepper motors drive the stage under computer control. The computer control is achieved by a custom computer program which makes it possible for the

stage to undergo very complicated motions. Located in the path of the ablated laser plume, in between the target and substrate, is a partial shield that covers half of the stage when the stage is in the neutral position. This allows for precise control over which area of the substrate is deposited on, granting a combinatorial way to control in-situ thickness variations on a single substrate. As the substrate is moved in the y-direction to make the different CdTe thicknesses it is also constantly scanning in the x-direction (in and out of the page in Fig. 6) to achieve uniform thickness across the entire substrate. Thicknesses of 1.5, 1.25, 1.0, and 0.75 μm were chosen to be deposited on top of the 120 nm thick CdS layer. The schematic is depicted in figure 9.

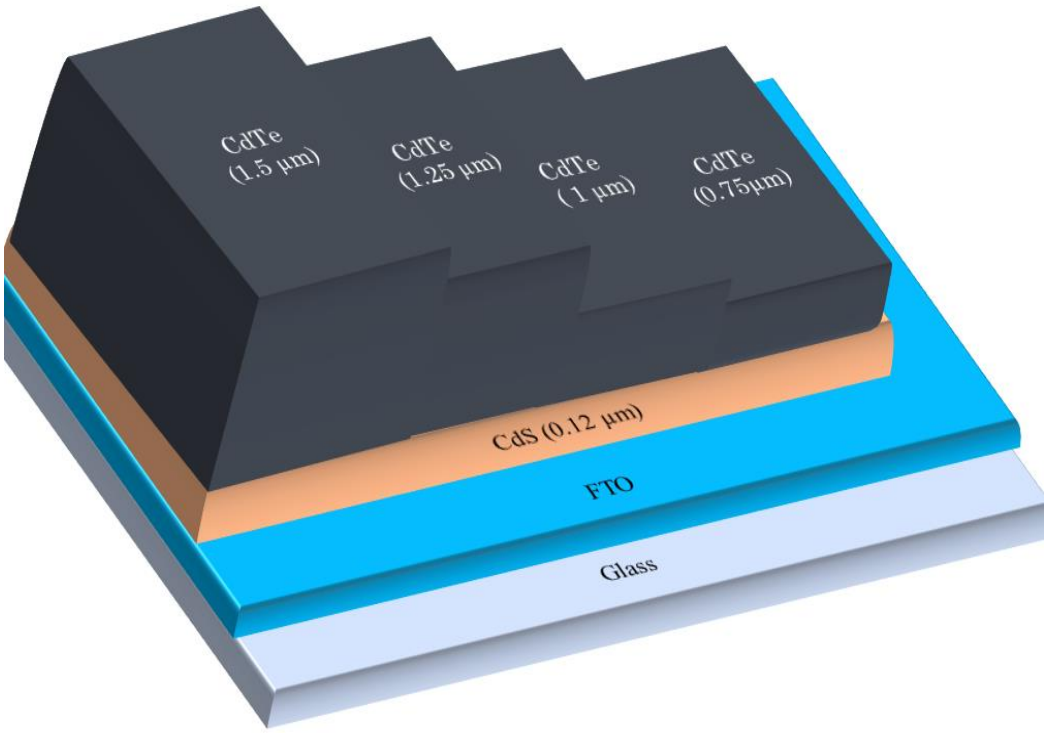

Figure 9: A schematic drawing of the samples made with varying CdTe thickness.

TEC 15 soda lime glass is used as the conductive substrate and serves as the front contact to the devices. The CdS window layer was deposited at 200 ^{o}C in 1.5 mTorr of Argon gas flow with a laser repetition rate of 10 Hz, spot size of 8.7 mm^2, and pulse energy of 150 mJ with a 0.3 OD filter reducing the energy to 70 mJ. The CdTe absorber layer parameters are identical except the laser spot size is decreased to 7.6 mm^2 and the thickness is varied in 250 nm steps from 750 nm to 1500 nm using the partial shield and moving stage. After ablation is complete, the sample was annealed in the vacuum chamber at 400 ^{o}C for 5 min in 20 Torr Ar and cooled naturally overnight to room temperature. In these conditions, two groups of samples were fabricated for comparison: sample A regards those not treated with ex situ $CdCl_2$ annealing after the PLD deposition, while sample B were exposed to the vapors of $CdCl_2$ at 360 ^{o}C, in mixed O_2 and Argon (25 sccm:100 sccm) for (10, 12, 15, and 17 minutes). The best result was obtained of sample B that was treated with 15 minutes. Therefore, the comparisons of physical properties are made between the samples A and B to elucidate the effect of the annealing on the solar cells of variable thicknesses of CdTe film. Figure 10 shows the real photos of the PLD.

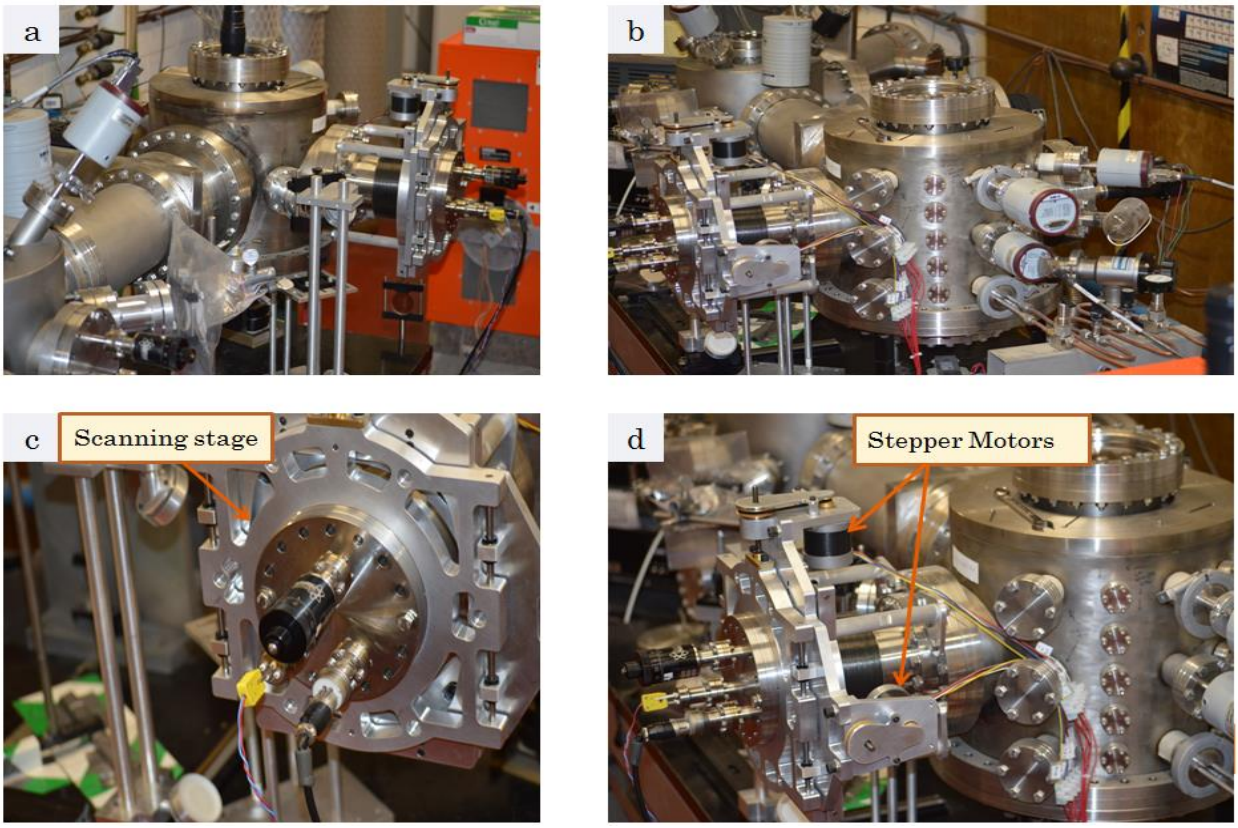

Figure 10: Real photos of PLD. Figures 10a and 10b represent PLD from both sides. Figures 10c and 10d are the scanning stage and two stepper motors respectively.

3.2.2 Cadmium Chloride ($CdCl_2$) Treatment

Achieving higher electric conversion efficiencies of (TCO/CdS/CdTe) solar cells requires a Cadmium Chloride ($CdCl_2$) treatment. This treatment, which is used on CdTe, is found to be extremely important in different aspects, such as helping in grain growth, blocking the channels or pinholes, and increasing the majority carriers in CdTe [16-18]. There are several ways in which cadmium chloride ($CdCl_2$) has been used as a treatment of the CdS/CdTe solar cell in order to achieve high conversion efficiency. For instance, some researcher groups have mixed the cadmium chloride powder with methanol and spread it on the CdTe solar cell. They leave the solvent until evaporated, and then the new structure will be treated at certain conditions

(atmosphere, temperature and duration). In addition, the thickness of CdTe is various, so that the duration of $CdCl_2$ treatment will be various, as thicker films require longer treatment. After this process and due to the white color of $CdCl_2$, the surface of CdTe, which has a dark color, will turn out milky. Other researchers have used different methods, such as laser ablation and vacuum evaporation to deposit cadmium chloride as a layer on CdS and CdTe respectively [42-45]. Currently, $CdCl_2$ treatment with a Freon gas, such as (HCF2CL), which consists of Chlorine, has been used as another treatment, and solar cells with conversion efficiencies close to 16% have been achieved[46].

In this thesis, the $CdCl_2$ treatment has been done as following; 50mL of methanol and 0.075 g of $CdCl_2$ powder have been mixed together. The solution was dropped on the piece of glass and warmed to 98-100 ^{o}C until the source dried on the glass. After that, the solar cell sample (TCO/CdS/CdTe) was flipped face down on the source of $CdCl_2$. Figure 11 shows this process. Then, the sample was placed into the tube furnace.

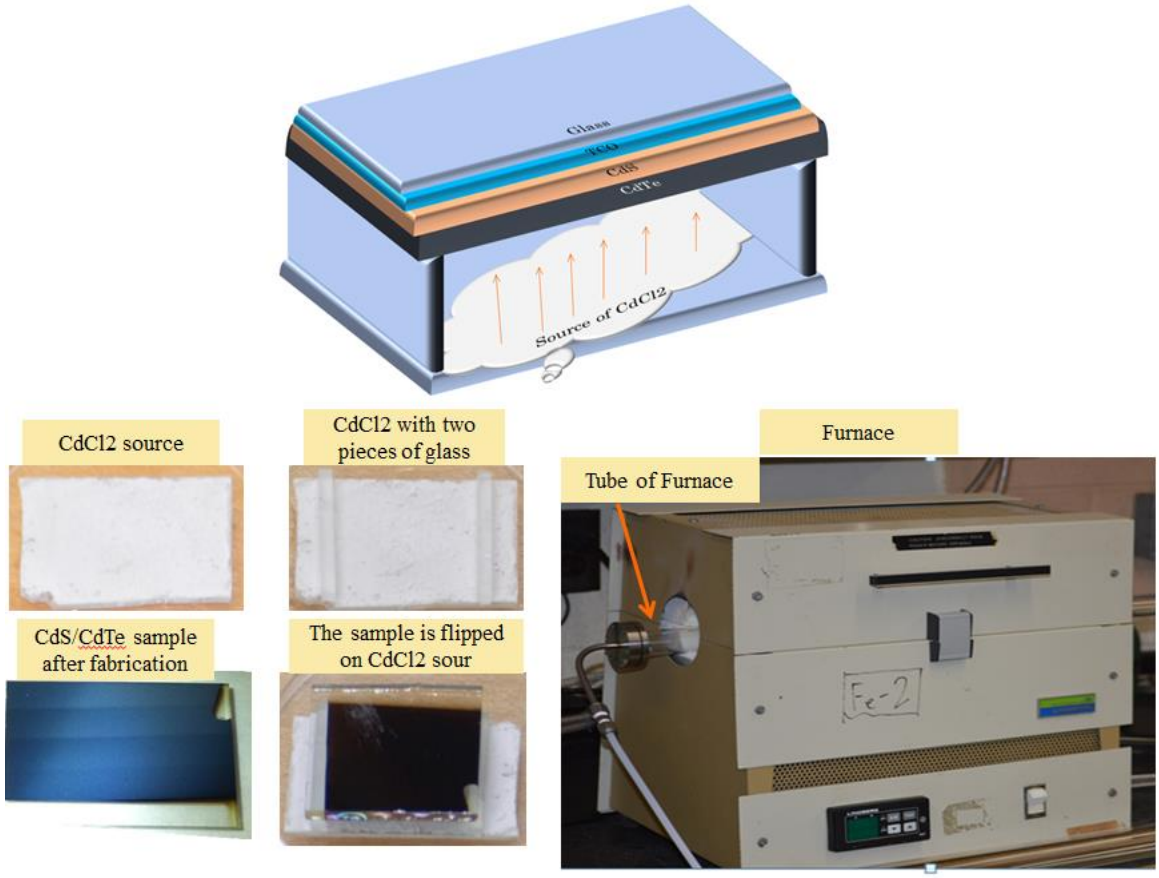

Figure 11: Process of CdCl2 treatment.

Groups of sample B were exposed to the vapors of $CdCl_2$ at 360 ^oC, in mixed O_2 and Argon (25 sccm:100 sccm) at 10, 12, 15, and 17 minutes. The best result was obtained of sample B that was treated at 15 minutes. Therefore, the comparisons of physical properties are made between the samples A and B to elucidate the effect of the annealing on the solar cells of different thicknesses of CdTe layer.

3.2.3 Electrical Back Contacts

In the solar cell fabrication, using a metal on the CdTe is an important step to provide an electrical back contact. The contact between metal and semiconductor will have a resistance higher than connection between two metals [3, 9]. In other words, the metal's work function is

the required energy to remove an electron from the Fermi Level to the vacuum. On the other hand, the work function of semiconductor can be controlled by doping. Particularly, when semiconductor is doped p-type, will have a work function greater than when it is doped n-type [3]. Therefore, there are no metals with work functions greater than or similar to the work function of p-type CdTe semiconductor[3]. Table 2 shows the work function of the p-type CdTe and some materials that have been used as an electrode.

Table 2: Work functions of CdTe, gold, cooper, and silver

p-type CdTe	5.9 eV
Ag	4.7 eV
Au	5.1 eV
Cu	4.65 eV

In other words, metal-p type semiconductor junction tends to form a Schottky barrier, and it is a significant challenge to provide a low resistance ohmic contact instead. As a result, many researchers have tried to reduce this barrier by producing a mixture of some materials that can have a work function between the metal and CdTe semiconductor [47]. This material is called the back contact, and the most popular back contact (B. C.) used in the CdTe solar cell is a mixture of Copper, Mercury Telluride, and Graphite which has a work function (~5.3). Appling the (B.C.) requires the surface of CdTe to be Te-rich in order to reduce the series resistance so that another step has to be done before the (B.C.) which is called Bromine etching. The etching process is used to remove contaminants from the surface as well as make a Te-rich surface for better ohmic contact [27]. Studies are already underway to resolve this issue.

In this work, the samples were etched using the Bromine: Methanol. The Bromine etch is produced by mixing 0.25 mL Bromine with 25 mL Methanol. The sample was submerged for 4 seconds and then immediately rinsed with Methanol, Acetone, and IPA. Small contacts with average areas of roughly 1.25 mm^2 are then applied across the entire sample. The contact paste is made using Cu doped HgTe (0.017 g Cu, 4 g HgTe, 10 g graphite paste). After application, the sample is baked in the tube furnace with 100 sccm Ar flow at 280^oC for 30 minutes. Then the electrode (Silver) was coated on the back contact, and the sample also baked at 150 ^oC for 60 minutes. Figure 12 shows the final structure of FTO/CdS/CdTe.

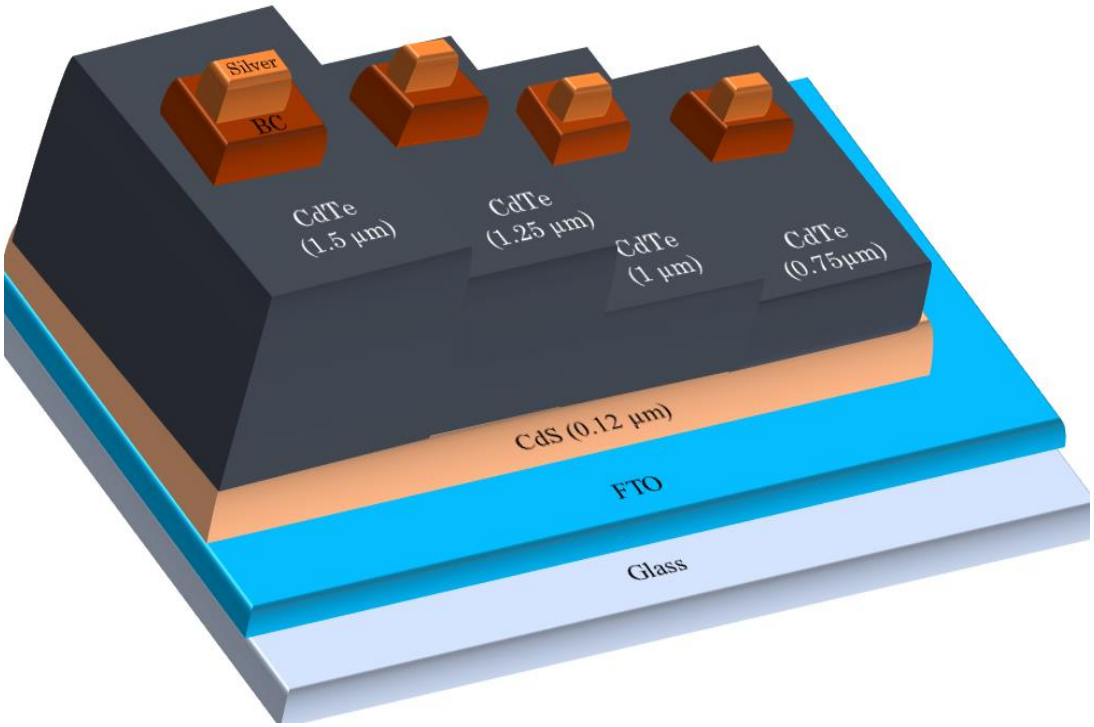

Figure 12: Final structure of FTO/CdS/CdTe solar cell.

3.3 Microstructural Measurements

Atomic force microscopy (AFM) and Raman spectroscopy (488 nm excitation wavelength) were performed using a WiTec Alpha 300 confocal Micro Raman system to obtain surface roughness and phase orientation for the different growth and annealing conditions.

3.4 Electrical Measurements

Current-voltage (I-V) measurement from which the performance of the solar cell can be determined, such as open circuit voltage, short circuit current, fill factor, and the conversion efficiency. Figure 13 shows the I-V curve measurement.

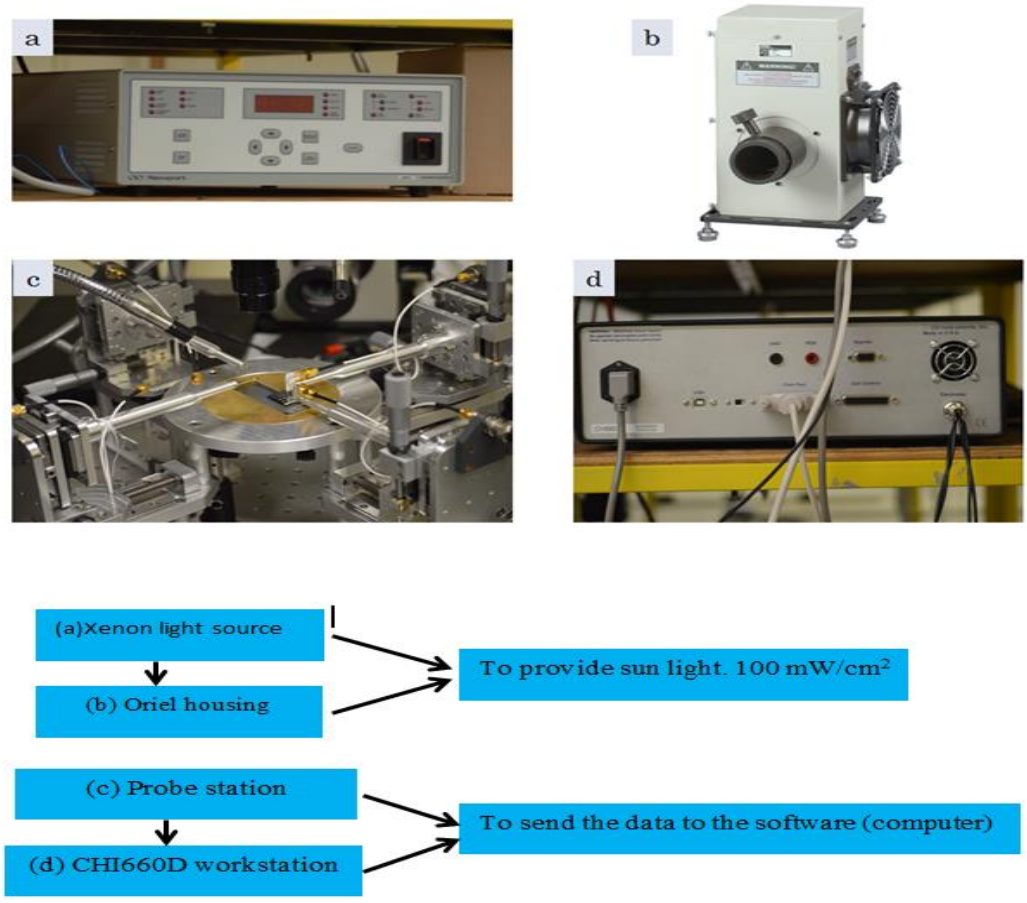

Figure 13: Current-Voltage (I-V) measurement.

Current density-voltage curves were measured under an AM 1.5 solar simulator of 100 mW/cm^2 photo optic lamp by using a Newport solar simulator with Oriel housing at room temperature as shown in figure 13a and 13b.Two probes were used to connect both of the front and back contacts of the solar cell by utilizing a probe station as shown in figure 13c. The probes connect to the CHI660D electrochemical workstation to send the data to the computer in order to calculate the I-V curve.

The quality of the materials and the perfect solar cell design can be obtained by measuring the quantum efficiency (QE), which represents the ratio between the numbers of electrons collected by the solar cell to the number of photons incident on the solar cell [3, 29]. Figure 14 shows a system of QE Measurement.

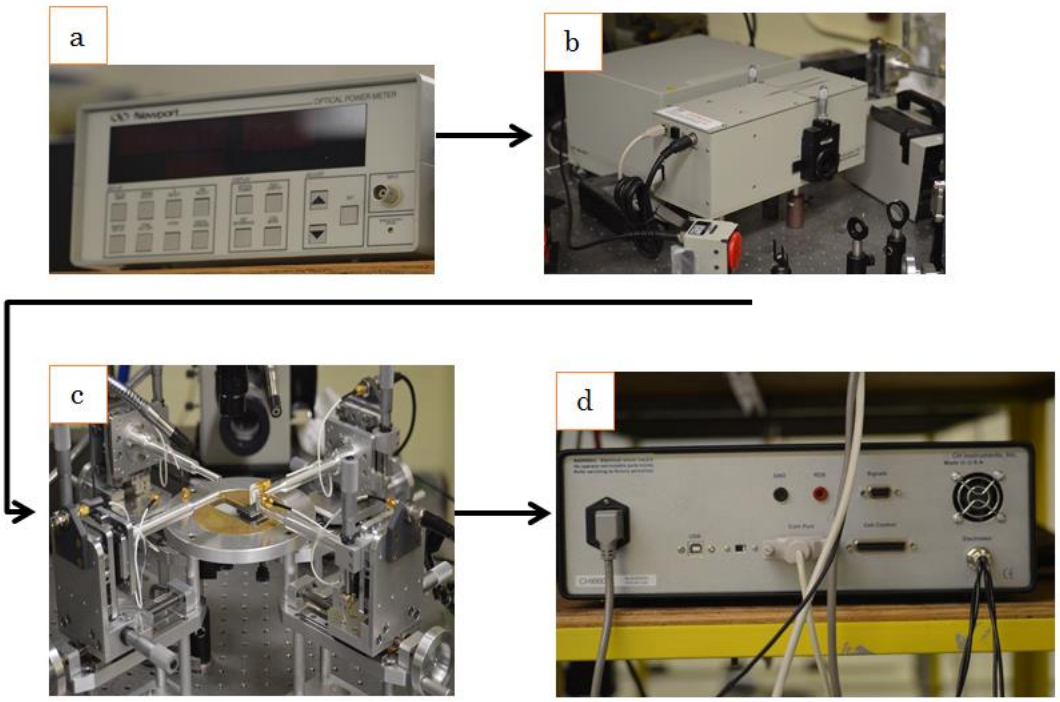

Figure 14: Quantum efficiency measurement system.

Figure 14 shows the external quantum efficiency EQE measurements. Figure 14a represents a Newport Optical Power which provides a power to Newport monochromator in order to select wavelengths. The monochromatic light output is focused on a test cell by optical lenses as shown in figure 14b. The sample is already placed on the probe station and connected to the CHI660D electrochemical workstation. The previous procedure will be repeated for the sample under measurement[48]. The current from the solar cell, which is measured under illumination, is used to calculate the number of electrons generated due to photovoltaic effect. Also, the current of the standard reference solar cell provides the number of photons. TracQ Basic software calculates instrument control, data collection and calculations.

Chapter 4. Results and Discussion

For comparison, five groups of samples were fabricated using combinatorial Pulsed Laser Deposition (cPLD) by which the variable thickness of CdTe were obtained l.5, 1.25, 1.0, 0.75 μm in correspondence to layers 1, 2, 3, and 4 respectively on the same substrate. Sample A regards those not treated with ex situ $CdCl_2$ annealing after the cPLD deposition, while the other samples were exposed to the vapors of $CdCl_2$ at 360 ^oC, and they were treated with different durations of $CdCl_2$ 10, 12, 15, and 17 minutes respectively. Sample B that was treated at 15 minutes $CdCl_2$ showed the best performance in all thickness range 0.75-1.5 μm. Therefore, comparisons of physical properties were made between the samples A and B to elucidate the effect of the annealing on the solar cells with variable thicknesses of CdTe.

4.1 Microstructural Results

4.1.1 Atomic force microscopy (AFM)

Atomic force microscopy (AFM) was applied to characterize the CdTe surface morphology before and after $CdCl_2$ treatment. The results are compared in figure 15 for samples without (sample A) and with (sample B) 15 minutes $CdCl_2$ annealing. The AFM images indicate that the average roughness and the grain size of the CdTe in sample A are in the range of 13-16 nm and 140-160 nm, respectively. The crystallinity and grain size of this sample is very small and one might expect there is still much recombination in a device made with this CdTe as there would still be many grain boundaries. The deposition at low temperature (200 ^oC) is not sufficient enough to promote good grain growth. On the other hand, in sample B, the average roughness for all layers was roughly 30 nm and the grain size is much larger which can clearly be observed in

the second row of the AFM images. There is a correlation between the grain size seen at the film surface and the thickness of CdTe. This is most easily seen in sample B where it is obvious that the grains get bigger as the thickness gets smaller. The thinnest layer of CdTe at 0.75 μm has grains that vary in size from 300-700 nm while the thickest layer at 1.5 μm has grains in the range of 150-550 nm. The average grain size for the thinnest layer is approximately 65% of the total thickness. For the thicker layer the average grain size is closer to 20% of the total thickness. This difference seen in grain size per thickness is most likely because the recrystallization is easier in the thinner layers as there is less material. As expected the $CdCl_2$ annealing promotes recrystallization and additional grain growth, which is shown by the improvements in surface roughness and grain size.

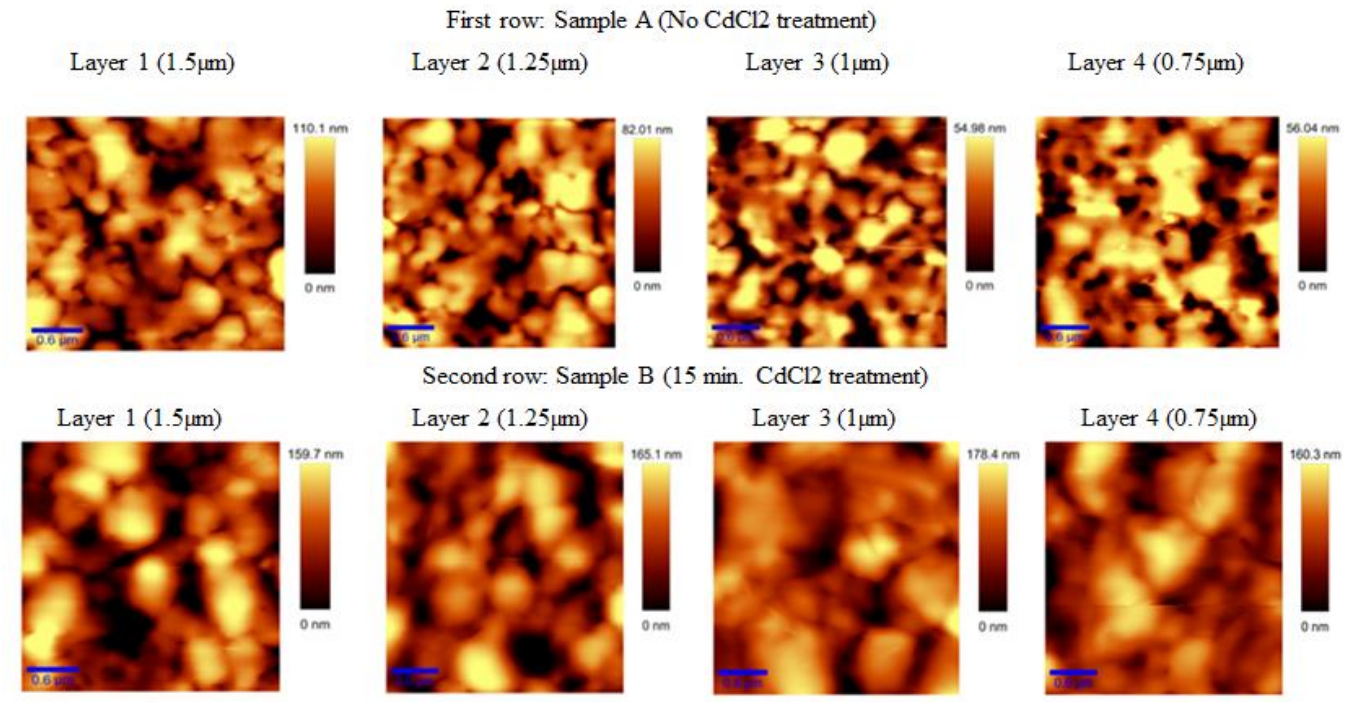

Figure 15: First row of AFM images is corresponding to sample A (No CdCl2 annealing). The second row is corresponding to the sample B (with 15 min. CdCl2 annealing). The scale bar for all images is 0.6 μm.

4.1.2 Raman Spectroscopy

Raman spectroscopy was performed in order to examine the structural properties between the two samples and the data can be seen in Figure 16. The transverse optical phonon (TO) for CdTe is known to be located at a Raman shift of 141 cm^{-1}, which can clearly be seen in all of the plots. The peak at the 169 cm^{-1} shift is assigned to the longitudinal optical phonon (LO) of CdTe[49]. The peaks at 292 cm^{-1} and 750 cm^{-1} are attributed to the 2TO mode of CdTe and tellurium oxide (TeO_x), respectively [50, 51]. The TeO_x signature found in both samples is possibly attributed to oxygen residues which might exist during the fabrication of the samples. By comparison of the two samples, it is obvious that the peaks of sample A have lower intensities compared to sample B, which was processed with the 15 minute $CdCl_2$ treatment. This indicates that there is an improvement in the crystallinity of the CdTe after the annealing.

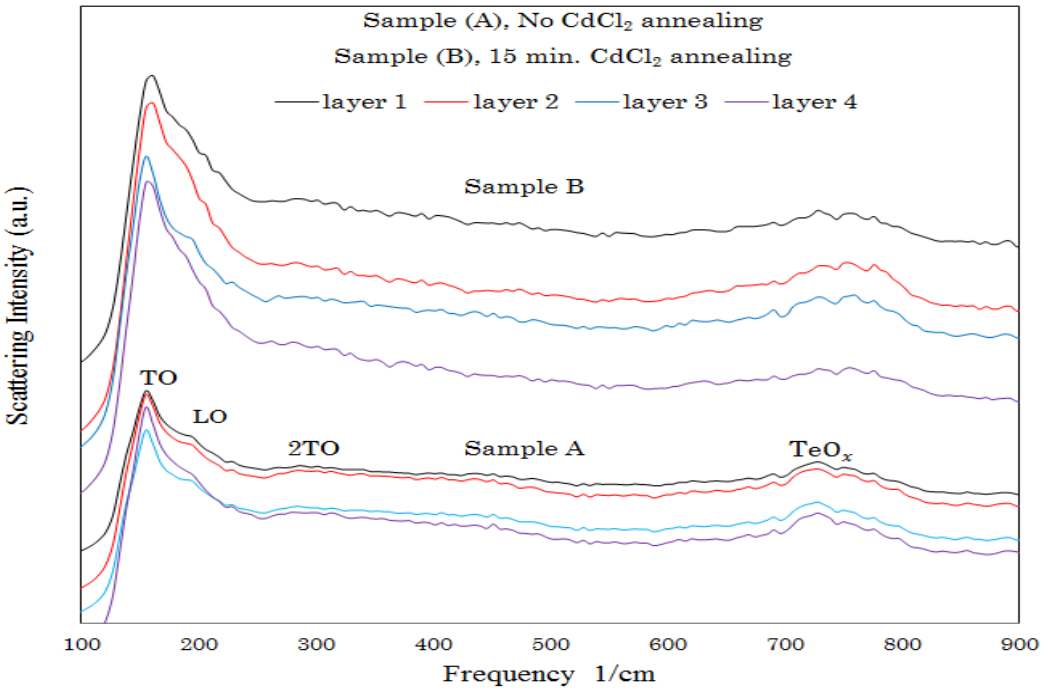

Figure 16: Raman spectroscopy of sample A and B.

The selection rules for CdTe illustrates that the TO and LO modes of CdTe are allowed from (110) and (100), respectively. Also, both modes can be allowed from (111).[52-54]. The LO mode is not highly pronounced after $CdCl_2$ annealing suggesting that the polycrystalline structure of sample B is in the (110) crystal orientation.

4.2 Current- Voltage (J-V) Results

Figure 17 shows the J-V curves of the highest performance of variable thicknesses CdTe for the two samples made with and without $CdCl_2$ treatment. The JV data from sample B shows that the best performance came from the thinnest CdTe layer of 0.75 μm. This layer achieved a maximum efficiency of 5.3% with a J_{SC}, V_{OC}, and FF of 17.6 mA/cm^2, 643 mV, and 45%, respectively. Obviously this layer will absorb the fewest photons due to its thickness in accordance with the Beer-Lambert Law. However, the shortest travel distance for charges to be collected at the electrodes may outweigh the loss in photon absorption as compared to its thicker counterparts. The data from all cells can be seen in Tables 3 and 4, which are the averages of the four cells made on each layer. Note that the JV curves are the best performing cells from each layer.

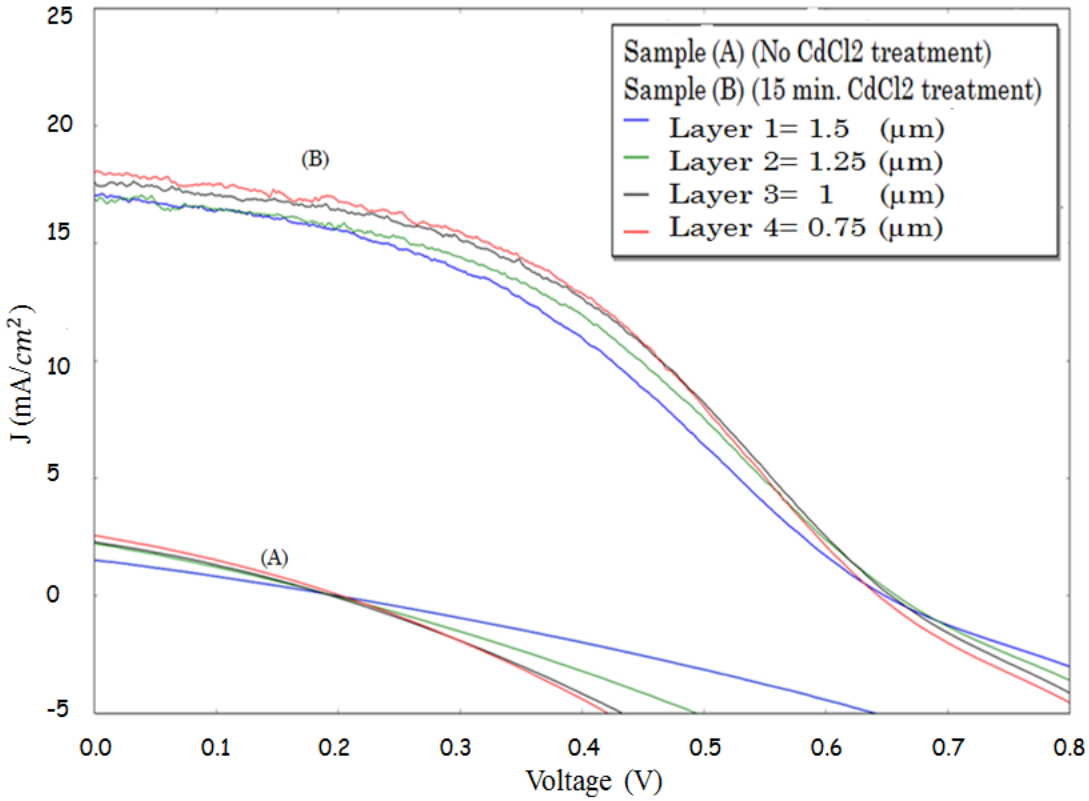

Figure 17: Current-Voltage (J-V) curves of the two sample A and B.

All of the layers in sample A have extremely low performance as one would expect. The extremely small V_{oc} is attributed to the weak electric field established by the p-n junction, due to the lack of doping in CdTe which is achieved during the $CdCl_2$ annealing process, and quite possibly pinhole formation. The CdTe for this sample is possibly nanocrystalline, which causes huge amounts of recombination due to the small grain sizes [55, 56]. This would affect not only the fill factor, but the J_{sc} as well. The order of magnitude increase in the J_{sc} of sample B is due to the increased number of majority carriers, improvements in the grain connectivity, and increases in the grain size, which implies a reduced density of the grain boundaries. However, the rollover seen in sample B indicates that the series resistance which occurs due to the contact between materials is still high.[27] This is a matter of optimization between the CdTe, back contact, and electrode and studies are already underway to resolve this issue.

4.3 Performance of CdS/CdTe Solar Cells

Table 3: Thicknesses and electrical properties of sample A with No CdCl2 annealing.

Sample A	Layer 1	Layer 2	Layer 3	Layer 4
Thickness of CdS (µm)	0.12			
Thickness of CdTe (µm)	1.5	1.25	1	0.75
V_{OC} (mV)	214	198	203	197
J_{SC} (mA/cm^2)	1.7	2.5	2.6	3.0
FF %	27	28	29	29
Efficiencies %	0.10	0.14	0.15	0.18

Table 4: Thicknesses and electrical properties of sample B with 15 minutes CdCl2 annealing.

Sample B	Layer 1	Layer 2	Layer 3	Layer 4
Thickness of CdS(µm)	0.12			
Thickness of CdTe(µm)	1.5	1.25	1	0.75
V_{OC} (mV)	638	639	645	651
J_{SC} (mA/cm^2)	16.5	16.7	17.0	18.0
FF %	36	39	42	45
Efficiencies %	4.0	4.2	4.6	5.1

Figure 18 shows how the key parameters of the solar cells change as a function of thickness. The V_{oc} is essentially unchanged regardless of the CdTe thickness indicating that the same or comparable charge doping level, and thus the built-in bias voltage, was achieved in all layers. The J_{sc} values are also nearly identical between the layers of different thickness regardless of whether they were processed with or without the $CdCl_2$ annealing. However, a 690% fold increase in of the J_{sc} value was observed in samples with $CdCl_2$ annealing with respect to their counterparts without such annealing. The biggest factor contributing to difference in performance between layers was the FF. There is a linear decrease in FF observed with increasing CdTe thickness. The higher FF values seen at smaller CdTe thicknesses indicate the benefit of less recombination at smaller CdTe thickness as expected.

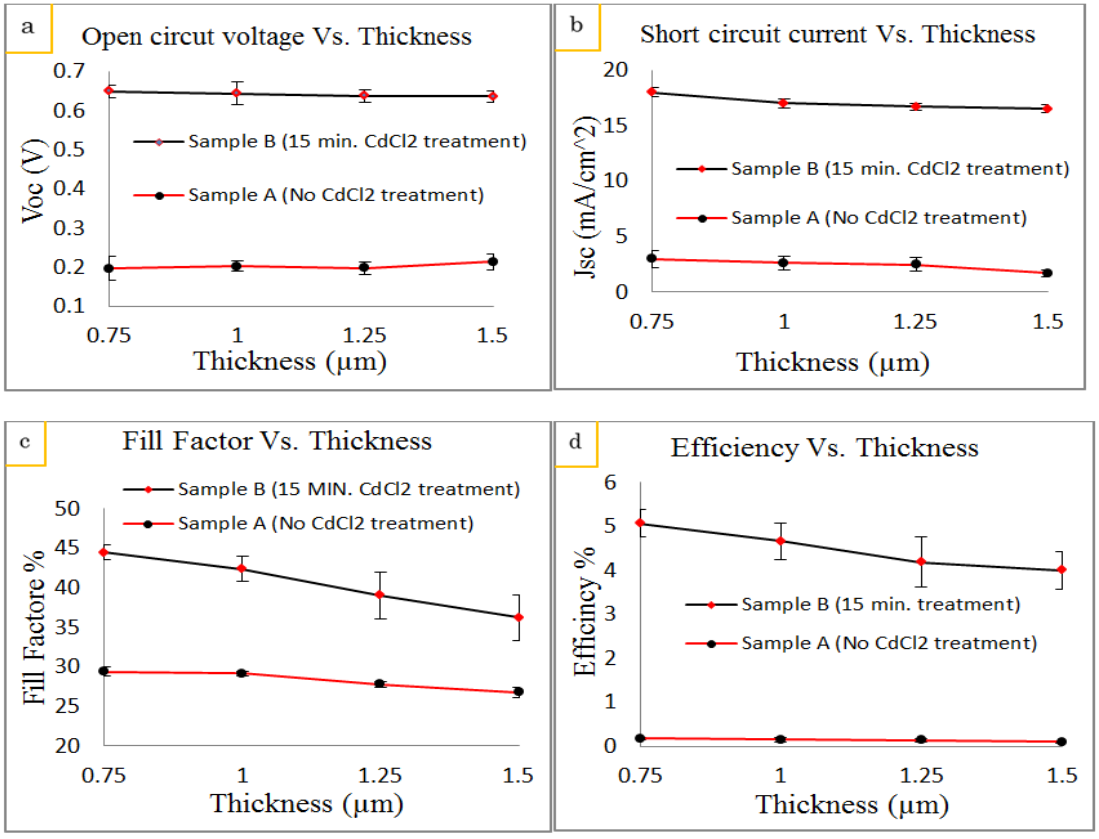

Figure 18: The values of open circuit voltage (a), short circuit current (b), fill factor (c), and efficiency (d) as a function of CdTe thickness.

4.4 External Quantum Efficiency Results

The efficiency of the solar cell can be further characterized by measuring the external quantum efficiency EQE, which represents the ratio between the numbers of electrons collected by the solar sell to the number of photons incident on the solar cell.[57]

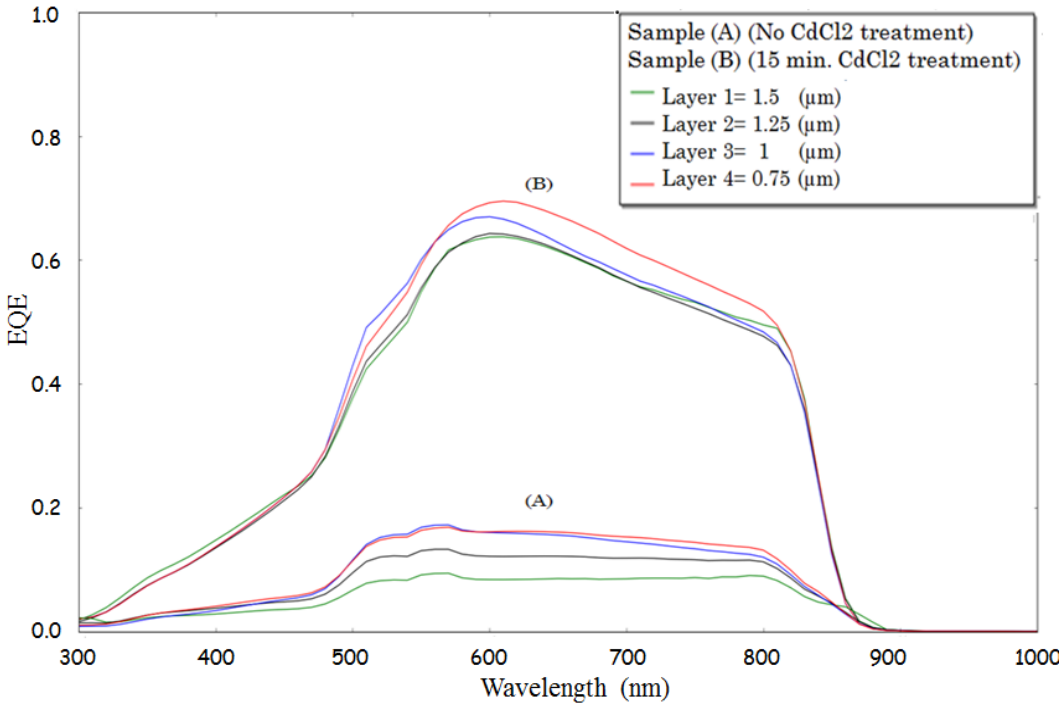

Figure 19: The quantum efficiencies for the best performing cells from the two samples made with (B) and without (A) CdCl2 annealing.

Figure 19 shows the extreme difference in the EQE between samples A and B. The EQE of sample B is much higher than that of sample A which indicates that the probability of collection has been improved after the $CdCl_2$ treatment. We also gain more insight into the behavior between the different CdTe thicknesses. The two thickest CdTe layers in sample B have nearly identical EQE curves implying that the recombination relative to CdTe thickness is the same for these two layers. When reducing the CdTe thickness from 1.25 µm to 1 µm an improvement in EQE was observed. An even further increase in EQE was observed when

reducing the thickness by another 250 nm to 0.75 μm. The entire increase in collection efficiency from layer 3 to layer 4 happens above the CdS band edge. This observation, combined with the comparable grain size revealed in AFM and crystallinity in Raman analysis, clearly indicates that the thinnest layer is the better performer because of less recombination in the CdTe due to the decreased number of grain boundaries encountered by electrons/holes in this cell. This observation is important in further optimization of the thin film CdS/CdTe solar cells.

Conclusion

CdS/CdTe solar cells with variable thickness were fabricated using cPLD system. Five samples were fabricated with one sample not being treated with $CdCl_2$ annealing. The other four samples were treated in $CdCl_2$ vapor at 360 °C for different durations of 10, 12, 15, and 17 minutes, respectively. The sample that was treated at 15 minutes $CdCl_2$ showed the best performance in all thickness range 0.75-1.5 μm. The effects of the $CdCl_2$ treatment increased doping, improved grain connectivity, and created larger grains in the CdTe. The AFM images show that the average roughness and the grain size of sample A (No $CdCl_2$ annealing) in the range 13-16 nm and 140-160 nm respectively, implying that the grain sizes are still too small and the grain boundaries are massive. However, after the $CdCl_2$ treatment (sample B), the roughness becomes in the range of 28-30 nm and the grain size increases to 350-450 nm. The increase in grain size implies a reduced density of the grain boundaries which led to a reduction in charge recombination. In addition, Raman spectra show that the CdTe signature peaks intensities have been increased after the $CdCl_2$ treatment, and this also promotes the crystallinity of the CdTe. These improvements led to a significant increase in the performance (V_{oc}, J_{sc}, FF, and η) of the CdTe solar cells. The grain size of ~450 nm in the sample B yield the best power conversion efficiency 5.3% in the solar cells of the thinnest CdTe layer of 0.75 μm, it most probably was due to the benefit of reduced charge recombination outweighing the reduced optical absorption.

References

1. A.Romeo, A.N.T., H Zogg, M. Wagner, J.R. Guenter. *Influence of Transparent Conducting Oxides on the Properties of CdTe/CdS Solar Cells Proceedings of 2nd World Conference and Exhibition* in *Photovoltaic Solar Energy Conversion*. 6-10 July 1997. Vienna (Austria), 1105-1108.
2. Bube, A.L.F.R.H., *Fundamentals of Solar Cells, Photovoltaic Solar Energy Conversion*. Academic Press, INC. (London) LTD.
3. Nelson, J., *The Physics of Solar Cells*. 2004, UK: Imperial College Press. 363.
4. APS Physics, T.M.i.P.H. *Bell Labs Demonstrates the First Practical Silicon Solar Cell*. [cited 2015; Available from: APS Physics
5. Kazmerski, L.L., *Photovoltaics: A review of cell and module technologies.* Renewable and Sustainable Energy Reviews, 1997. **1**(1–2): p. 71-170.
6. Singh, J., *Physics of Semiconductor Devices (Book).* Physics Today, 1990. **43**(10): p. 98.
7. L. Frantzis, E.J., A. N. D. Little, C. Lee, M. Wood, and P. Wormser. . *In Proceedings of 16th European Photovoltaic Solar Energy Conference*. 2000. Glasgow, United Kingdom.
8. Neamen, D.A., *Semiconductor Physics and Devices*. 2003: McGraw-Hill Higher- Education, Elizabeth A. Jones.
9. EDUCATION.ORG, P. *Semiconductor Structure*. [cited 2015 05/13]; Available from: PV EDUCATION,OGR.
10. Electronics, P.a.R. *Deplation Region*. [cited 2015 5/24].
11. Jenny, D.A. and R.H. Bube, *Semiconducting Cadmium Telluride.* Physical Review, 1954. **96**(5): p. 1190-1191.
12. Cusano, D.A., *CdTe solar cells and photovoltaic heterojunctions in II–VI compounds.* Solid-State Electronics, 1963. **6**(3): p. 217-218.
13. Tyan, Y.S., *Polycrystalline thin film CdS/CdTe photovoltaic cell*. 1980, Google Patents.
14. NREL, N.R.E.L. *Polycrystalline Thin-Film Materials and Devices R&D, CdTe Research*. [cited 2015 5/25]; Available from: National Renewable Energy Laboratory NREL,.
15. Nakayama, N., et al., *Ceramic Thin Film CdTe Solar Cell.* Japanese Journal of Applied Physics, 1976. **15**(11): p. 2281.
16. Abdul-Manaf, N.A., et al., *Development of Polyaniline Using Electrochemical Technique for Plugging Pinholes in Cadmium Sulfide/Cadmium Telluride Solar Cells.* Journal of Electronic Materials, 2014. **43**(11): p. 4003-4010.
17. Baron, B.N., et al., *Polycrystalline thin film materials and devices*. 1992. p. Medium: ED; Size: Pages: (107 p).
18. Moutinho, H.R., et al. *Studies of recrystallization of CdTe thin films after CdCl₂ treatment [solar cells]*. in *Photovoltaic Specialists Conference, 1997., Conference Record of the Twenty-Sixth IEEE*. 1997.
19. PV FAQs. *Will we have enough materails for energy-significant PV production*. [cited 2015; Available from: PV FAQs.
20. Gupta, A., V. Parikh, and A.D. Compaan, *High efficiency ultra-thin sputtered CdTe solar cells.* Solar Energy Materials and Solar Cells, 2006. **90**(15): p. 2263-2271.
21. Krishnakumar, V., et al., *A possible way to reduce absorber layer thickness in thin film CdTe solar cells.* Thin Solid Films, 2013. **535**(0): p. 233-236.
22. Salavei, A., et al., *Influence of CdTe thickness on structural and electrical properties of CdTe/CdS solar cells.* Thin Solid Films, 2013. **535**(0): p. 257-260.

23. *First Solar sets new world record for CdTe solar cell efficiency*. 2013.
24. Green, M.A., et al., *Solar cell efficiency tables (version 42).* Progress in Photovoltaics: Research and Applications, 2013. **21**(5): p. 827-837.
25. Qiao, Q., et al., *A comparison of fluorine tin oxide and indium tin oxide as the transparent electrode for P3OT/TiO2 solar cells.* Solar Energy Materials and Solar Cells, 2006. **90**(7–8): p. 1034-1040.
26. Baek, W.-H., et al., *Use of fluorine-doped tin oxide instead of indium tin oxide in highly efficient air-fabricated inverted polymer solar cells.* Applied Physics Letters, 2010. **96**(13): p. 133506.
27. Fang, Z., et al., *Achievements and Challenges of CdS/CdTe Solar Cells.* International Journal of Photoenergy, 2011. **2011**: p. 8.
28. Wu, X., *High-efficiency polycrystalline CdTe thin-film solar cells.* Solar Energy, 2004. **77**(6): p. 803-814.
29. EDUCATION.ORG, P. *Quantum Efficiency* [cited 2015; Available from: PV EDUCATION,OGR.
30. EDUCATION.ORG, P. *short circuit current*. [cited 2015 05/13]; Available from: PV EDUCATION,OGR.
31. EDUCATION.ORG, P. *Open Circuit voltage* [cited 2015 05/13]; Available from: PV EDUCATION,OGR.
32. EDUCATION.ORG, P. *Fill Factor*. [cited 2015 05/13]; Available from: PV EDUCATION,OGR.
33. EDUCATION.ORG, P. *the efficiency* [cited 2015 05/13]; Available from: PV EDUCATION,OGR.
34. EDUCATION.ORG, P. *Shunt Resistance* [cited 2015; Available from: PV EDUCATION.ORG.
35. EDUCATION.ORG, P. *Seriese resistance* [cited 2015 05/13]; Available from: PV EDUCATION,OGR.
36. *Handbook of photovoltaic science and engineering, 2d ed.* Reference and Research Book News, 2011. **26**(2).
37. Bing, L., et al., *Development of pulsed laser deposition for CdS/CdTe thin film solar cells.* Applied Physics Letters, 2012. **101**.
38. Harrison, P., et al., *The effects of fabrication pressure on the physical properties of CdS/CdTe thin film solar cells made via pulsed laser deposition.* Photovoltaic Specialists Conference (PVSC), 2013 IEEE 39th, 2013.
39. Meeth, J., et al., *Pulsed Laser Depositin of Thin Film CdTe/CdS Solar Cells with CdS/ZnS Superlattice Window.* Photovoltaic Specialists Conference (PVSC), 2013 IEEE 39th, 2013.
40. Moure-Flores, F.d., et al., *Physical properties of CdTe:Cu films grown at low temperature by pulsed laser deposition.* Journal of Applied Physics, 2012. **112**.
41. Pengchen, H., et al., *Effects of the substrate temperature on the properties of CdTe thin films deposited by pulsed laser deposition.* Surface and Coatings Technology, 2012. **213**.
42. Komin, V., et al., *The effect of the CdCl2 treatment on CdTe/CdS thin film solar cells studied using deep level transient spectroscopy.* Thin Solid Films, 2003. **431–432**(0): p. 143-147.
43. Metzger, W.K., et al., *CdCl2 treatment, S diffusion, and recombination in polycrystalline CdTe.* Journal of Applied Physics, 2006. **99**(10): p. 103703.
44. Potter, M.D.G., et al., *A study of the effects of varying cadmium chloride treatment on the luminescent properties of CdTe/CdS thin film solar cells.* Thin Solid Films, 2000. **361–362**(0): p. 248-252.
45. Romeo, N., et al., *A highly efficient and stable CdTe/CdS thin film solar cell.* Solar Energy Materials and Solar Cells, 1999. **58**(2): p. 209-218.
46. Mazzamuto, S., et al., *A study of the CdTe treatment with a Freon gas such as CHF2Cl.* Thin Solid Films, 2008. **516**(20): p. 7079-7083.
47. Granek, F. and C. Reichel, *Back-contact back-junction silicon solar cells under UV illumination.* Solar Energy Materials and Solar Cells, 2010. **94**(10): p. 1734-1740.

48. Newport. *QEPVSI-b Quantum Efficiency Measurement System*. [cited 2015 5/26]; Available from: Newport, QEPVSI-b Quantum Efficiency Measurement System.
49. Kimata, M., et al., *Interdiffusion of In, Te at the interface of molecular beam epitaxial grown CdTeInSb heterostructures.* Journal of Crystal Growth, 1995. **146**(1–4): p. 433-438.
50. Dewan, N., et al., *Growth of amorphous TeOx(2≤x≤3) thin film by radio frequency sputtering.* Journal of Applied Physics, 2007. **101**(8): p. 084910.
51. Wang, D., Z. Hou, and Z. Bai, *Study of interdiffusion reaction at the CdS/CdTe interface.* Journal of Materials Research, 2011. **26**(5): p. 697-705.
52. Amirtharaj, P.M. and F.H. Pollak, *Raman scattering study of the properties and removal of excess Te on CdTe surfaces.* Applied Physics Letters, 1984. **45**(7): p. 789-791.
53. Islam, S.S., et al., *Forbidden one-LO-phonon resonant Raman scattering and multiphonon scattering in pure CdTe crystals.* Physical Review B, 1992. **46**(8): p. 4982-4985.
54. Menéndez, J., et al., *Resonance Raman scattering in CdTe-ZnTe superlattices.* Applied Physics Letters, 1987. **50**(16): p. 1101-1103.
55. Kosyachenko, L.A., E.V. Grushko, and V.V. Motushchuk, *Recombination losses in thin-film CdS/CdTe photovoltaic devices.* Solar Energy Materials and Solar Cells, 2006. **90**(15): p. 2201-2212.
56. Maniscalco, B., et al., *The activation of thin film CdTe solar cells using alternative chlorine containing compounds.* Thin Solid Films, (0).
57. Nelson, J., *The physics of solar cells*. 2003, Imperial College Press.